• Basic Research •

Atorvastatin-induced neuroprotection against NMDA-induced retinal excitotoxicity: association with altered retinal PPARα and PPARγ expression

Jing Yi Wong[1], Heethal Jaiprakash[1,2], Renu Agarwal[2], Igor Iezhitsa[2], Purushotham Krishnappa[2], Siew Tung Wong[2], Maxim A. Perfilev[3], Pavel M. Vassiliev[3]

[1]School of Post Graduate Studies, IMU University, Bukit Jalil, Kuala Lumpur 57000, Malaysia
[2]School of Medicine, Department of Pathology and Pharmacology, IMU University, Bukit Jalil, Kuala Lumpur 57000, Malaysia
[3]Research Center of Innovative Medicines, Volgograd State Medical University, Pavshikh Bortsov sq. 1, Volgograd 400131, Russian Federation
Correspondence to: Heethal Jaiprakash. School of Medicine, IMU University, Bukit Jalil, Kuala Lumpur 57000, Malaysia. heethaljp@gmail.com
Received: 2025-12-31 Accepted: 2026-09-16

Abstract

● **AIM:** To explore the effect of atorvastatin on the retinal expression of peroxisome proliferator-activated receptors (PPARs) and its anti-apoptotic and pro-survival effects against excitotoxic retinal injury.

● **METHODS:** An *in-silico* study was conducted to determine the affinity of statins towards PPARs and the one with maximum affinity was chosen for further studies. Rats were intravitreally administered with N-methyl-D-aspartate (NMDA), with or without statin pre-treatment, at doses ranging from 0.1 to 100 µmol/L. Retinal Bcl-2-associated X protein (BAX), Bcl2, caspase-3, RNA-binding protein with multiple splicing (RBPMS) expressions were determined to assess pro-apoptotic and pro-survival effects. To further corroborate the findings, haematoxylin & eosin (H&E)-stained retinal sections were examined to evaluate retinal morphology. Furthermore, the effect of atorvastatin on retinal expression of PPARs in the presence and absence of excitotoxic injury was determined.

● **RESULTS:** Among the six statins, atorvastatin demonstrated the highest affinity towards PPARα and PPARγ receptors. Among five doses, atorvastatin at a dose of 20 µmol/L dose showed the most significant reduction in BAX/Bcl-2 and cleaved/procaspase-3 ratios (P<0.0001). RBPMS expression and morphological studies confirmed the most prominent protective effect of atorvastatin at 20 µmol/L dose. Additionally, this optimum dose of atorvastatin inhibited NMDA-induced changes in retinal PPARα and PPARγ expression.

● **CONCLUSION:** Atorvastatin prevents NMDA-induced retinal cell apoptosis and promotes retinal ganglion cell survival in rats. This effect of atorvastatin is associated with inhibition of NMDA-induced changes in retinal PPARα and PPARγ expression. Importantly, this study not only highlights the role of PPARs in the neuroprotective effect of atorvastatin but also demonstrates contrasting effects of excitotoxic injury on retinal PPAR expression under these experimental conditions.

● **KEYWORDS:** statins; NMDA; peroxisome proliferator-activated receptors; excitotoxicity; apoptosis; dose-response; glaucoma

DOI:10.18240/ijo.2026.12.06

Citation: Wong JY, Jaiprakash H, Agarwal R, Iezhitsa I, Krishnappa P, Wong ST, Perfilev MA, Vassiliev PM. Atorvastatin-induced neuroprotection against NMDA-induced retinal excitotoxicity: association with altered retinal PPARα and PPARγ expression. *Int J Ophthalmol* 2026;19(12):2360-2372

INTRODUCTION

Retinal ganglion cell (RGC) loss and optic nerve degeneration are characteristic features of glaucomatous neuropathy, a leading cause of irreversible blindness. Although, precise pathophysiology underlying the neuronal loss in glaucoma remains debatable, the role of glutamate-induced excitotoxicity is widely recognised. Glutamate is the principle excitatory neurotransmitter in the retina. The transmission of visual information from photoreceptors to bipolar cells, then to RGCs, and finally to brain centres involves glutamate-mediated neurotransmission *via* its multiple receptors[1]. One of the glutamate receptor subtypes, the N-methyl-D-aspartate (NMDA) receptor, is primarily implicated in glaucomatous RGC loss. There is evidence suggesting that there is

endogenous glutamate build-up leading to excessive glutamate receptor activation in glaucomatous retina[2-3]. Moreover, adult RGCs are susceptible to NMDA administered exogenously, and inhibitors of NMDA receptors and/or downstream pathways protect neurons in experimental models of retinal ischemia, excitotoxicity and glaucoma[4].

Interestingly, the role of peroxisome proliferator-activated receptors (PPARs), in the pathophysiology of various neurological disorders has attracted research interest over recent years. Both PPARα and PPARγ subtypes are widely expressed in all retinal layers, including the ganglion cell layer (GCL), the site of RGC loss in glaucoma[5-6]. PPARα activation was shown to protect against ischemia-induced RGC apoptosis by suppressing activation of glial cells and neuroinflammation[6]. Similarly, PPARγ activation provided a neuroprotective effect in a rat model of optic nerve crush by inhibiting glial cell activation[7]. Evidence shows that PPARγ is also an important regulator of retinal neuroprotection. Its activation was shown to supress neuroinflammation, reduce oxidative stress, inhibit microglial activation, and attenuate RGC apoptosis in experimental models of retinal injury[6]. Furthermore, studies have indicated that statins modulate PPARγ signalling independent of the lipid lowering effect. Atorvastatin was shown to upregulate PPARγ expression and activity, leading to decreased inflammatory cytokine production, decreased oxidative stress, and enhanced neuronal survival[6,8]. In fact, statins, besides their popularly known lipid-lowering effect, have been shown to exert the neurotrophic function *via* the PPARα–CREB pathway, and the importance of PPARα in the therapeutic success of simvastatin in an animal model of Alzheimer's disease has been described[9]. In a retrospective longitudinal cohort study, a lower incidence of primary open angle glaucoma (POAG) was observed among those on statins compared to those not on statins[10]. Additionally, statin use was shown to be associated with the stabilisation of visual field progression in patients with normal tension glaucoma and open angle glaucoma[11-13]. Other studies have also shown that various statins, including pravastatin, rosuvastatin, lovastatin, atorvastatin, and fluvastatin, protect RGCs from ischemia/reperfusion injury and optic nerve injury[9,14-15]. However, the direct protective effect of statins against NMDA-induced retinal cell injury remains unclear.

Since one of the determinants of the efficacy of ligands is their affinity for target receptors, in this study, we determined the integral affinity of six statins, including atorvastatin, fluvastatin, lovastatin, pravastatin, rosuvastatin, and simvastatin, towards PPARα and PPARγ, and created docking spaces for multiple compounds on these receptors. By integrating these methods, we aimed to develop a comprehensive understanding of the receptor-binding profiles and the pleiotropic effects of statins. Next, we carried out *in vivo* studies using several doses of the statin that showed maximum efficacy towards PPARs, to investigate its anti-apoptotic and pro-survival effects against NMDA-induced retinal cell apoptosis. By developing a log dose-response curve for anti-apoptotic effect, the 50% effective dose (ED_{50}) and ED_{95} were calculated, which were used in the next set of experiments that delineated the effect of atorvastatin on retinal expression of PPARs in the presence and absence of excitotoxic injury. Although previous studies have shown the neuroprotective effect of statins in various neurodegenerative disorders, their protective effect against NMDA induced retinal excitotoxicity remains to be established *in vivo*. Hence, the novelty of the study lies in evaluating the effect of atorvastatin, beyond its well-known lipid lowering effect, against for NMDA-induced retinal injury in rats. This study not only highlights the role of PPARs in the neuroprotective effect of atorvastatin but, to the best of our knowledge, is also the first study to demonstrate contrasting effects of excitotoxic injury on retinal PPAR expression under these experimental conditions.

MATERIALS AND METHODS

Ethical Approval This study was conducted in compliance with the ARVO statement for the use of animals for ophthalmic and vision research[16] and the animal ethics guidelines of IMU University. The study was approved by IMU Joint-Committee on Research and Ethics [MMHS I-2023(01)].

In this study we first carried out an *in-silico* study to determine the affinity of various statins towards PPAR. The statin that showed the maximum affinity was then subjected to *in vivo* studies. The first set of *in vivo* study aimed to determine its optimum dose of chosen statin in preventing the NMDA-induced RGC loss. The subsequent *in vivo* study determined the effect of the optimum dose on NMDA-induced changes in retinal PPAR expression.

***In-silico* Study to Determine the Affinity of Statins Towards PPARs** To perform the *in-silico* study, the data on the 2D structures of six statins, including atorvastatin, fluvastatin, lovastatin, pravastatin, rosuvastatin, and simvastatin, were employed. Additionally, two experimental X-ray crystallographic 3D models of the PPARα and PPARγ were used. For data processing and analysis, various computer programs were used. Chemical structure information was processed using ChemOffice 9.0[17]. Compound conformers were constructed through molecular mechanics methods with MarvinSketch 17.1.23[18], while optimisation of compound conformations was performed using quantum chemistry methods using MOPAC2012[19]. Spaces for multiple docking were constructed with MSite 23.10.4[20], and multiple docking itself was carried out with AutoDock Vina 1.1.1[21]. Furthermore, fully connected neural correlation networks

were constructed and trained using CorrConv 24.1.24, and general data processing was handled with MS Office Excel 2013[22]. All computations for this research were executed on a high-performance supercomputer with a cluster architecture, achieving a peak performance of approximately 31.2 teraflops.

Construction of sets of optimized 3D conformers of the investigated compounds The structural formulas of fluvastatin, lovastatin, pravastatin, rosuvastatin, and simvastatin were retrieved from the DrugBank database[23]. We generated 10 conformers with the lowest energy for each of these six compounds using molecular mechanics methods in the MarvinSketch 17.1.23 program[18]. Subsequently, the constructed conformers underwent optimisation through the MOPAC2012 program[19] utilising the semi-empirical quantum chemical method PM7. In total, 60 optimised conformers were generated.

Selection of valid 3D models of PPARα and PPARγ Valid experimental X-ray crystallographic models of PPARα and PPARγ of Homo sapiens were retrieved from the International Union of Basic and Clinical Pharmacology (IUPHAR) database[24]. The files with their 3D structure were obtained using the UniProt[25] and PDBe[26] databases. The valid 3D models of PPARα and PPARγ of Homo sapiens were included in the ligand-binding domain.

Construction of spaces for multiple docking of compounds into PPARα and PPARγ The docking simulations were conducted using the original MSite 23.10.4 program[20]. Within the entirety of each protein's 3D model, 27 equally sized spaces were constructed, facilitating the docking of compounds across various regions of the biomolecule. An earlier study by Vasilyev *et al*[20] demonstrated that the energy matrix resulting from multiple docking is a significantly more robust metric of ligand affinity to pharmacologically relevant biomolecules compared to the energy vector obtained from simple docking into the binding site alone. This approach allows for the consideration of the collective effect of a set of ligand molecules on the entire protein structure.

Multiple docking of conformers of investigated compounds into PPARα and PPARγ The AutoDock Vina 1.1.1 program[21] was utilised to conduct multiple docking of all 60 optimised 3D conformers of the six studied compounds into each of the 27 spaces within the 3D models of PPARα and PPARγ. Data processing was executed in stream mode, employing custom scripts tailored for this purpose. For each 3D model of PPARα and PPARγ and each original conformer of the six compounds under study, docking was performed five times, each time in a new calculation. In each calculation, analysis was conducted on the ten most favourable biological ligand conformations within the binding space, determining the conformation with the minimum docking energy ΔE for the given original conformer in the binding space. In total, thus, an array of 2×27×6×10×5×10=162 000 processed.

Subsequently, for each of the ten original conformers of each of the six compounds, a spectrum of 135 minimum docking energies, ΔE values, was obtained (5×27). Based on these values, twelve affinity matrices (6 ligands in 2 targets) were constructed for subsequent neural network modelling. Each matrix reflected the overall affinity of each of the six compounds to PPARα or PPARγ, comprising 1350 values of minimum docking energies ΔE (a total of 16 200 values).

Construction of fully connected neural correlation networks based on multiple docking data of statins and calculation of their integral affinity to PPARα and PPARγ The concept of a simple neural network was proposed by Hebb[27] in 1949. Based on this concept, Hopfield[28] in 1982 developed an architecture of a fully connected neural network with a symmetric matrix of connections[28], in which neurons are binary X_i={1, -1}, and network training is carried out by minimising a functional called network energy

$$E = \frac{1}{2}\sum_{\substack{i,j=1 \\ i\neq j}}^{M} w_{ij}\cdot X_i \cdot X_j \qquad (1)$$

where M—the number of neurons (variables); w_{ij}—weights of synapses (interneuronal connections).

With a large number of neurons, minimising the functional, Equation 1 becomes computationally very complex. In addition, the Hopfield network can only be constructed and trained on binary variables. This study develops and applies a new architecture for a fully connected artificial neural correlation network. In this network, the neurons X_i are real numbers, and training, *i.e.*, the calculation of weights w_{ij}, is performed by calculating the coefficients of pairwise correlations:

$$R_{ij}\frac{Cov_{ij}}{S_i \cdot S_j}, i,j = 1 \ldots M, i \neq j \qquad (2)$$

$$R_{ij}=R_{ji}$$

where Cov_{ij} is the sample covariance of variables X_i and X_j, and S_i, S_j are the sample standard deviations (SD) of variables X_i and X_j, respectively.

Under these conditions, the energy W of the fully connected neural:

$$W = \sum_{l=1}^{N} W_l = \sum_{l=1}^{N}\frac{1}{2}\sum_{\substack{i,j=1 \\ i\neq j}}^{M} R_{ij}\cdot X_{il}\cdot X_{jl} \qquad (3)$$

where N is the number of objects (observations) with dimensionality M; W_l is the energy of object l; X_{il}, X_{jl} are the values of variables i, j for observation l.

Construction of landscapes of integral affinity of the statins to PPARα and PPARγ Using the Statistica 7.0 program[29],

separate construction of two energy landscapes W_{kl} of fully connected neural correlation networks was performed for each PPARα and PPARγ receptor, for l=1…10 conformers of each of k=1…6 statins. A comparative landscape of energy W_k of fully connected neural correlation networks for k=1…6 statins were jointly constructed for PPARα and PPARγ.

Anti-apoptotic and Pro-survival Effects of Statins Against NMDA-Induced Retinal Cell Apoptosis *in vivo* Sprague Dawley rats of either sex, aged 8–12wk, and weighing 200–250 g, were sourced from A Sapphire Enterprise, Selangor, Malaysia. The rats were kept under standard laboratory conditions with a 12-hour light-dark cycle. Food and water were available *ad libitum*. Before inclusion in the study, all animals underwent general examination and baseline ophthalmic examination. The ophthalmic assessment included inspection of the external ocular structures for abnormalities, including ocular discharge, conjunctival abnormalities and corneal opacity, only animals with no detectable ocular abnormalities were included in the study.

Atorvastatin was purchased from Selleckchem, Houston, USA, and the stock solution was freshly prepared at a concentration of 3 mmol/mL in 0.1% dimethyl sulphide (DMSO; Sigma-Aldrich, Missouri, USA) as the solvent and stored at -20°C. The stock solution was then diluted with 0.1% DMSO to achieve the desired concentrations of 0.1, 0.5, 1.0, 20, and 100 μmol/L.

Study design The first part of the *in vivo* study determined the optimum dose of atorvastatin for its anti-apoptotic effects, and subsequently, the effect of the optimum dose was studied on the expression of PPARα and PPARγ receptors.

A total of 126 rats were divided into seven groups of 18 animals each. Group 1 received no treatment, while Group 2 was given 0.1% DMSO as the vehicle. Groups 3 to 7 were administered with atorvastatin injections at concentrations of 0.1, 0.5, 1.0, 20, and 100 μmol/L, respectively. The dose range was extrapolated from previous studies[30-31]. After 24h of atorvastatin administration, Groups 2 to 7 were injected with 80 mmol/μL of NMDA to induce excitotoxicity. The dose of NMDA was in accordance with a previous study[32]. The animals were euthanised on day 7 post-injection with an overdose of sodium pentobarbital (100 mg/kg, Merck), eyes were enucleated, and the retinas were harvested. The retinal samples were processed for measurement of the Bcl2-associated X protein (BAX) and Bcl2 protein expression using enzyme-linked immunosorbent assay (ELISA). The expression of caspase-3 was determined using Western blot. The percent response for the anti-apoptotic effect of atorvastatin, measured by BAX/Bcl2 and cleaved/pro-caspase-3 ratios, was used to generate a log dose-response curve. The pro-survival effect of atorvastatin was evaluated by measuring retinal RNA-binding protein with multiple splicing (RBPMS) expression using Western blot and morphological studies using haematoxylin & eosin (H&E) staining. For each experimental group (n=18 rats), animals were divided into six biological subgroups of three rats each. The left retinae from the three rats within each subgroup were harvested, isolated, and pooled into a single sample (n=6). This pooling ensured an optimized, high-yield total protein concentration sufficient for multi-assay evaluation. One randomly chosen eye for each of the subgroups was enucleated intact as a representative sample and subjected to H&E staining. Finally, another set of experiment was conducted to delineate the effect of atorvastatin on retinal PPARα and PPARγ with and without excitotoxic injury using Western blot. Four groups of animals (n=9) received vehicle, NMDA, atorvastatin and atorvastatin pretreatment followed by atorvastatin. In this experiment, we used the ED_{95} determined by the log-dose response curve for the anti-apoptotic effect of atorvastatin. The retinas isolated 7d post-treatment were processed to measure PPARα and PPARγ expression using Western blot. For intravitreal injections, the animals were anaesthetised by an intraperitoneal injection of Zoletil® 100 (Virbac, Carros, France) with a 1:10 dilution and a dose of 3 mL/kg. The superior temporal sclera was punctured using a 30 G needle, and then injections were made slowly through the puncture using a 10 μL Hamilton syringe with a 30 G needle in a volume of 2 μL.

Enzyme-linked immunosorbent assay To determine BAX and Bcl2 protein expression, the retinae were first homogenised in 300 μL of commercial radioimmunoprecipitation assay (RIPA) lysis buffer (Abcam, Cambridge, UK) by sonication for 15s at 1/2 cycle with an amplitude of 60 μmol. The samples were incubated on ice for 15min and then centrifuged at 4°C at 13 000 rpm for 5min. The supernatants were collected and used for the assay.

Retinal BAX and Bcl2 levels were measured using commercially available assay kits (E-EL-R0098 and E-EL-R0096, respectively; Elabscience Biotech, Wuhan, Hubei Province, China) as per the manufacturer's protocol. Briefly, the rat BAX or Bcl2 biotinylated detection antibodies and the Avidin-horseradish peroxidase (HRP) conjugate were successively added to microplate wells designated for standards and samples. This was followed by incubation for 30min. The enzyme-substrate reaction was terminated with a sulfuric acid solution. The optical density (OD) was measured using a microplate reader (Infinite® 200 PRO, TECAN, Männedorf, Switzerland) at 450 nm. The target protein concentration in the samples was determined using the corresponding standard curves. All measurements were done in duplicate.

Western blot The Western blot was carried out using the western blot detection kit (E-IR-R304A, Elabscience Biotech, Wuhan, Hubei Province, China). Retinal samples were

Table 1 Antibodies used for Western blot analysis

Target	Antibody type	Catalog number	Size (kDa)	Dilution	Gel (%)	Source
RBPMS	Rabbit polyclonal	E-AB-91143	22	1:1000	15	Elabscience Biotech, China
Caspase 3	Mouse monoclonal	E-AB-22115	17	1:1500	15	Elabscience Biotech, China
PPARγ	Rabbit polyclonal	E-AB-70309	50	1:1000	12	Elabscience Biotech, China
β-actin	Mouse monoclonal	E-AB-84018	45	1:5000	12	Elabscience Biotech, China
PPARα	Rabbit polyclonal	A6697	52	1:1000	12	ABclonal Wuhan, China

RBPMS: RNA-binding protein with multiple splicing; PPAR: Peroxisome proliferator-activated receptor.

Table 2 Integral affinity of the studied compounds towards PPARα and PPARγ

Receptor	Network energy					
	Atorvastatin	Fluvastatin	Lovastatin	Pravastatin	Rosuvastatin	Simvastatin
PPARα	47471	16960	1021	2175	3189	2768
PPARγ	58258	5202	8458	22439	6187	-409

PPAR: Peroxisome proliferator-activated receptor.

processed as described for ELISA for protein extraction and then normalized to 0.75 mg/mL using 5× loading buffer.

For Western blot analysis, the gel was prepared according to the molecular weight of the proteins, and the corresponding gel concentrations are listed in Table 1. The gels were loaded with 7.5 μg of protein lysate. The electrophoresis was performed for 15min at 120 V for the stacking gel followed by 45min at 100 V for the resolving gel. The transfer of protein was done on a PVDF membrane for 120min at 100 V, then blocked with 5% skimmed milk for 1h at room temperature. Subsequently, the membranes were washed and incubated with corresponding antibodies (Table 1) overnight at 4°C on the orbital shaker. The membranes were washed and soaked in conjugated goat anti-rabbit/mouse secondary antibody (1:5000, Horseradish peroxidase, Elabscience Biotech, China). Protein bands were detected using ChemiDoc™ MP Imaging System (Bio-Rad Laboratories, California, USA). Image Lab 6.1 (Bio-Rad Laboratories, California, USA) was used to perform densitometry analysis of scanned films, and the results were expressed relative to the loading control (β-actin).

Retinal morphology The eyeballs were fixed in 10% formalin, were halved from the cornea to the optic nerve across the midline. Standard protocol for H&E staining was used for sample processing. The H&E-stained tissue sections of 4 μm thickness were viewed under a light microscope and were digitised using a whole-slide scanner (PANNORAMIC Midi II). Using the Slide Viewer software (DHISTECH Ltd., Budapest, Hungary), morphometric measurements were taken: 1 from close to the optic nerve, 2 from mid-periphery, and 2 from the periphery, as described earlier[33]. The parameters measured included thickness of the ganglion cell layer (GCL), thickness of the inner retina (IR), and the number of retinal cell nuclei along the GCL length in the field of vision. The means of these measurements were used to calculate a) the fractional thickness of the GCL within the IR, b) the fractional thickness of the GCL within the whole retina (WR), c) the ratio of IR to outer retina (OR), and d) the number of nuclei per 500 μm length of the GCL. The retinal cell nuclei count excluded endothelial and apparently non-neuronal cells, as described earlier[32,34-35]. Two independent and blinded observers made all measurements, and the average values from these measurements were used for statistical analysis.

Statistical Analysis All data were presented as means±SD from six independent samples (n=6). Statistical significance was determined using a one-way analysis of variance (ANOVA), followed by a post hoc Bonferroni analysis for multiple comparisons, using GraphPad Prism 10 for Windows. A P<0.05 was considered statistically significant.

RESULTS

Affinity of Statins Towards PPARs: *in-silico* Analysis Table 2 presents the integral affinity values of atorvastatin, fluvastatin, lovastatin, pravastatin, rosuvastatin, and simvastatin towards PPARα and PPARγ. These values are represented as the energy W of the neural fully connected correlation networks, which were constructed based on the multiple docking data of the 10 optimised conformers of each compound.

Based on the obtained integral affinity values, atorvastatin and fluvastatin are the most active towards PPARα, with atorvastatin exhibiting network energy values 2.80 times higher than fluvastatin for PPARα. Similarly, atorvastatin and pravastatin are the most active towards PPARγ receptors, with atorvastatin showing network energy values 2.60 times higher than pravastatin for PPARγ. Comparing affinities for both receptors, atorvastatin is 1.23 times more active towards PPARγ than PPARα. The other drugs show significantly lower affinity for both PPARα and PPARγ, with simvastatin showing almost no affinity for the PPARγ.

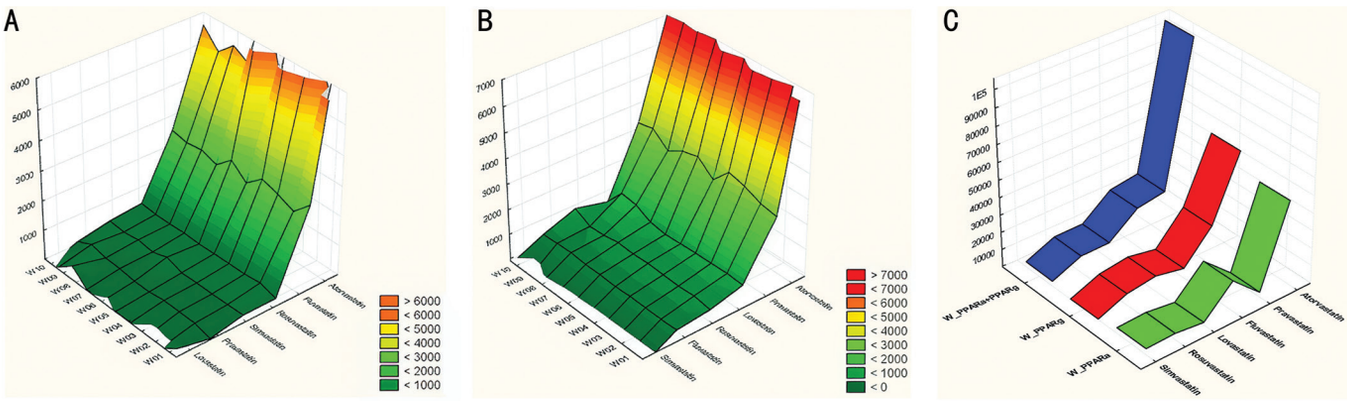


Figure 1 Affinity spectra and overall integral binding profiles of statins towards PPARα and PPARγ A: Spectra of integral affinity of statin conformers towards the PPARα receptor. The statins are ranked in terms of activity towards PPARα as follows: atorvastatin >> fluvastatin >> rosuvastatin ≈ simvastatin ≈ pravastatin > lovastatin; B: Spectra of integral affinity of statin conformers towards the PPARγ receptor. Ranking of statins by activity towards PPARγ based on the spectra of integral affinity of their conformers: atorvastatin >> pravastatin >> lovastatin > rosuvastatin ≈ fluvastatin >> simvastatin. This ranking corresponds well with the overall integral affinity values of the statins; C: Integral affinity of statins towards PPARα and PPARγ receptors. Landscape of overall integral affinity of statins, showing their ranking in combined PPARα and PPARγ pleiotropic activity based on cumulative energy of fully connected neural correlation networks: atorvastatin >> pravastatin ≈ fluvastatin > lovastatin ≈ rosuvastatin >> simvastatin. PPAR: Peroxisome proliferator-activated receptor.

According to the cumulative values of integral affinity, atorvastatin significantly outperforms all other statins by at least 4.30 times in terms of combined effect on both PPARα and PPARγ. However, fluvastatin and pravastatin are also quite active in terms of combined PPARα and PPARγ pleiotropic effects.

The energy landscape of fully connected neural correlation networks for statin conformers constructed for PPARα (Figure 1A) shows that, according to the spectra of integral affinity of the conformers, the statins are ranked in terms of activity towards PPARα as follows: atorvastatin >> fluvastatin >> rosuvastatin ≈ simvastatin ≈ pravastatin > lovastatin. This ranking agrees with the overall integral affinity values of the statins (Table 2).

The energy landscape of fully connected neural correlation networks for statin conformers constructed for PPARγ (Figure 1B) shows that, according to the spectra of integral affinity of the conformers, the statins are ranked in terms of activity towards PPARγ as follows: atorvastatin >> pravastatin >> lovastatin > rosuvastatin ≈ fluvastatin >> simvastatin. This ranking agrees with the overall integral affinity values of the statins (Table 2).

The landscape of overall integral affinity of statins (Figure 1C) shows that, based on the cumulative energy of fully connected neural correlation networks, the statins are ranked in terms of combined PPARα and PPARγ pleiotropic activity as follows: atorvastatin >> pravastatin ≈ fluvastatin > lovastatin ≈ rosuvastatin >> simvastatin, which is consistent with Table 2. Furthermore, the data reveal substantial class-wide variability in integral affinity values across both receptor subtypes. While certain statins, particularly atorvastatin, exhibit higher peak network energy levels for the PPARγ than the PPARα, the wide distribution of values, including negative affinity scores for specific statin for PPARγ, underscores distinct differences in ligand-receptor interaction dynamics rather than a uniform class effect.

Among the six statins subjected to *in-silico* analysis for their affinity for PPARs, atorvastatin showed maximum efficacy and hence was chosen for further investigations. To determine the anti-apoptotic effects of atorvastatin and various doses, first, we measured the retinal BAX and Bcl2 expression. The expression of caspase-3 was also measured to delineate the potential pathways to apoptosis. The protective effect of atorvastatin to promote RGC survival and protect retinal morphology was evaluated by measuring RBPMS and performing morphological studies. By analysing the dose-dependent anti-apoptotic effect of atorvastatin, we estimated the optimum dose of atorvastatin, and the effect of the optimum dose was studied on the retinal PPAR expression in the presence and absence of NMDA-induced injury.

Anti-apoptotic Effect of Atorvastatin Against NMDA-Induced Retinal Injury The retinal BAX expression in rats treated with NMDA was significantly higher compared to the untreated group (P<0.0001). However, in all atorvastatin-treated groups, BAX expression was significantly lower compared to the NMDA-treated group. Notably, in rats treated with atorvastatin, even with the lowest concentration of 0.1 μmol/L, the BAX expression was 1.81-fold lower than in the NMDA group (P<0.0001). At concentrations of 0.5, 1.0, 20, and 100 μmol/L atorvastatin caused a 2.39, 1.78, 3.27, and 2.07-fold lower retinal BAX expression compared to NMDA-treated group, respectively (P<0.0001; Figure 2A).

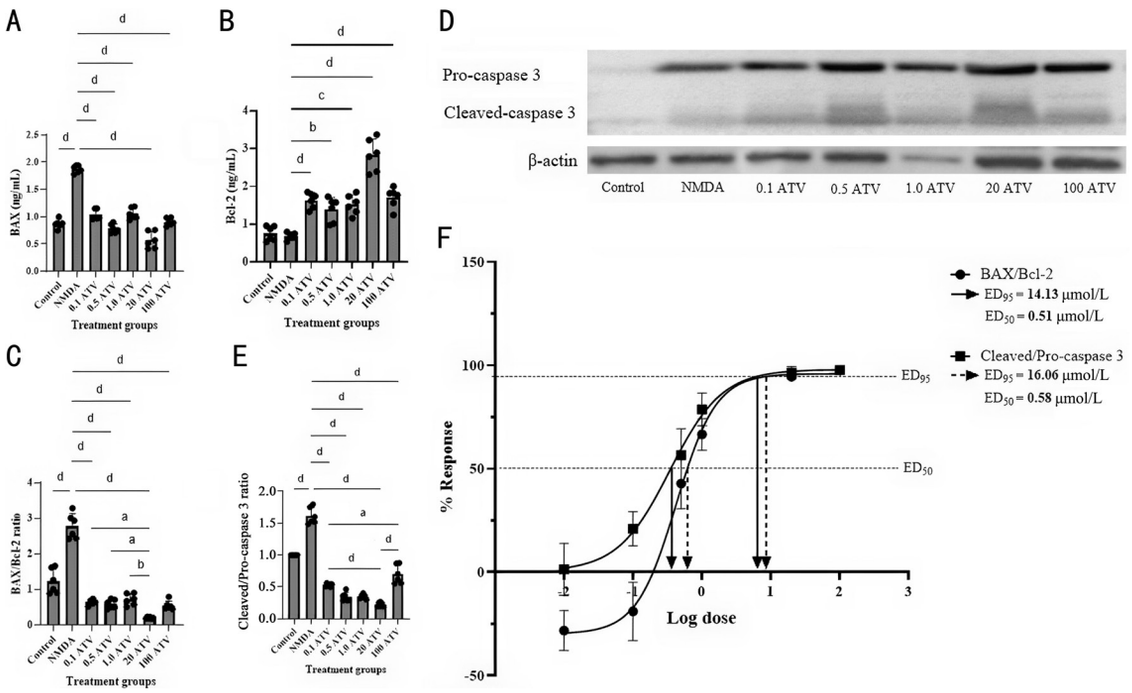


Figure 2 Anti-apoptotic effect of intravitreal administration of ATV at different doses against NMDA-induced retinal injury Statistical significance was analysed using one-way ANOVA with Bonferroni correction: [a]*P*<0.05, [b]*P*<0.01, [c]*P*<0.001, [d]*P*<0.0001. *n*=6. 0.1–100 on horizontal axis represents corresponding doses of ATV. A: BAX; B: Bcl2; C: BAX/Bcl2 ratio; D: Western blot bands showing caspase-3 expression; E: Densitometric estimation of Cleaved/pro-caspase-3 ratio; F: Log dose-response curve for the anti-apoptotic response of ATV. Each data point indicates the % response to different doses of ATV (0.1–100 µmol/L) against control. The values at lower doses are extrapolated to obtain a complete dose-resporse curve. ATV: Atorvastatin; NMDA: N-methyl-D-aspartate; ANOVA: Analysis of variance; BAX: Bcl-2-associated X protein.

We observed that the retinal Bcl2 protein expression in the NMDA-treated group remained comparable to that in the untreated group. However, the Bcl2 expression in all atorvastatin-treated groups was significantly greater than in the NMDA as well as the untreated groups. We observed 2.38, 202, 2.22, 4.13, and 2.49-fold greater Bcl2 expression at concentrations of 0.1, 0.5, 1.0, 20, and 100 µmol/L, respectively, compared to the NMDA-treated group (*P*<0.05; Figure 2B).

Further, we calculated the BAX/Bcl2 ratio in each of the groups. The NMDA group showed a significantly greater BAX/Bcl2 ratio compared to the untreated group. However, the retinal BAX/Bcl2 ratio was significantly lower in all atorvastatin groups compared to the NMDA-treated group, and the difference amounted to 4.32, 3.99, 3.64, 12.19, and 4.32-fold in 0.1, 0.5, 1.0, 20, and 100 µmol/L groups, respectively (*P*<0.0001). Moreover, the BAX/Bcl2 ratio was significantly lower in the group treated with atorvastatin 20 µmol/L compared to 0.1 and 1.0 µmol/L of atorvastatin (Figure 2C).

The retinal cleaved-caspase 3 expression in all atorvastatin-treated groups was lower than in the NMDA-treated group. The ratio of cleaved to pro-caspase-3 was significantly greater in the NMDA-treated group compared to the control group; however, the same ratio in all atorvastatin-treated groups was lower than the NMDA-treated group. Amongst all atorvastatin-treated groups, this ratio was smallest in the atorvastatin 20 µmol/L treatment group (Figure 2D and 2E).

Using the log of various atorvastatin doses used in this experiment and the corresponding % anti-apoptotic response measured by BAX/Bcl2 ratio and cleaved/pro-caspase-3 ratio, we obtained a log dose-response curve. As shown in Figure 2F, the ED_{50} for atorvastatin's effect on BAX/Bcl2 ratio and cleaved/pro-caspase-3 ratio was calculated to be 0.51 and 0.58 µmol/L, respectively, while ED_{95} for the same parameters was 14.13 and 16.06 µmol/L, respectively (Figure 2F).

Pro-survival Effect of Atorvastatin Against NMDA-Induced Retinal Injury The retinal RBPMS expression in rats treated with NMDA was significantly lower compared to the untreated group (*P*<0.0001). Although the RBPMS expression in all atorvastatin-treated groups remained lower than the control group, the group treated with atorvastatin 20 µmol/L showed a 1.53-fold higher RBPMS expression compared to the NMDA group (*P*<0.05; Figure 3A and 3B).

Examination of H&E-stained retinal sections under a light microscope revealed a thinner GCL and poor nuclear density with extensive vacuolations in the GCL of the NMDA-treated rats compared to untreated rats. The GCL in the retinal sections of atorvastatin-treated rats showed greater nuclear density and fewer vacuolations (Figure 3C). Morphometric estimations showed that the GCL thickness in the atorvastatin

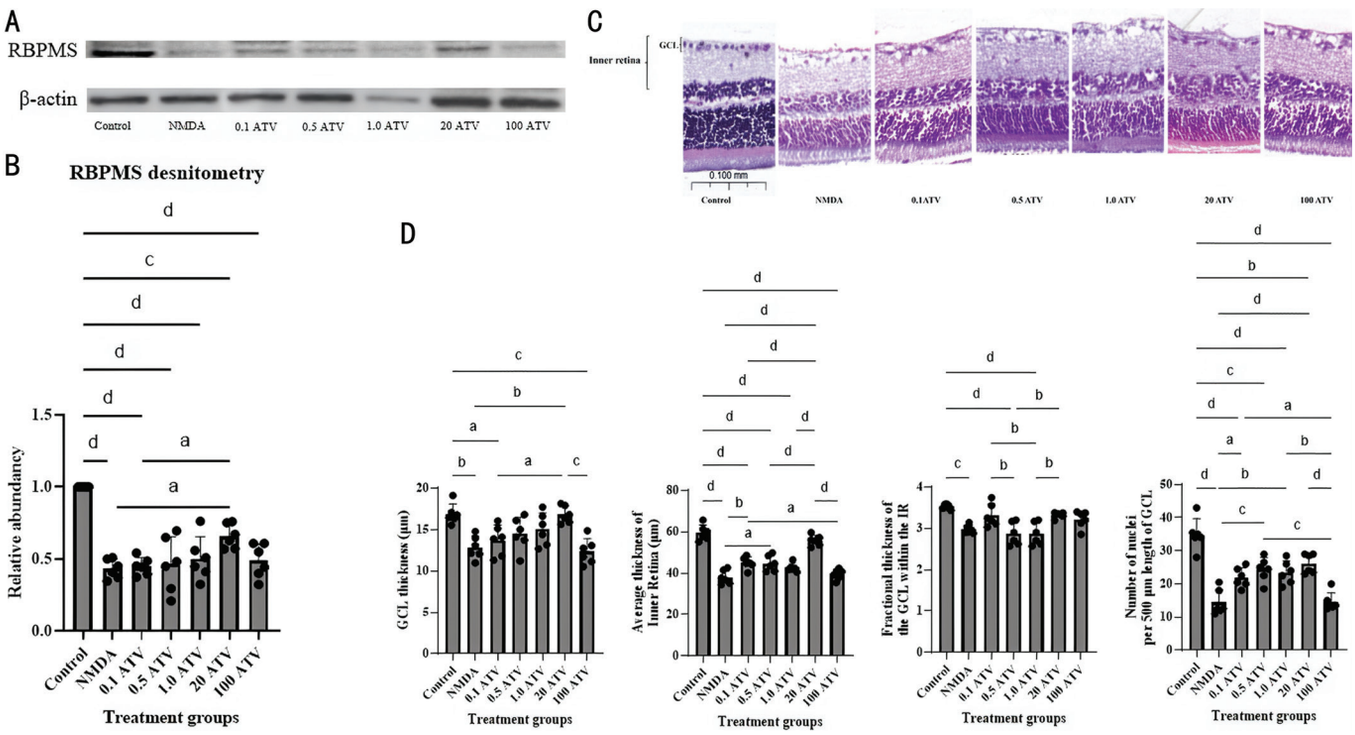


Figure 3 Pro-survival effect of intravitreal administration of ATV at different doses against NMDA-induced RGC loss and retinal morphological changes Statistical significance was analysed using one-way ANOVA with Bonferroni correction: [a]*P*<0.05, [b]*P*<0.01, [c]*P*<0.001, [d]*P*<0.0001. *n*=6. 0.1–100 on horizontal axis represents corresponding doses of atorvastatin. A: Western blot band showing RBPMS expression; B: Densitometric estimation of RBPMS expression; C: Representative photomicrographs of H&E-stained retinal sections; D: Morphometric estimations. ATV: Atorvastatin; NMDA: N-methyl-D-aspartate; GCL: Ganglion cell layer; ANOVA: Analysis of variance; IR: Inner retina; RBPMS: RNA-binding protein with multiple splicing.

20 μmol/L group was significantly higher than the NMDA group, and the difference amounted to 1.31-fold (*P*<0.001). The average thickness of the IR was 1.46-fold higher in the 20 μmol/L dose group of atorvastatin compared to the NMDA group (*P*<0.0001). Atorvastatin dose groups of 0.1 and 0.5 μmol/L also showed a 1.18-fold greater inner retinal thickness compared to the NMDA group (*P*<0.05). Among various atorvastatin dose groups, the one treated with 20 μmol/L showed significantly greater GCL thickness compared to those treated with 0.1 and 100 μmol/L. The mean IR thickness was significantly lower in the NMDA-treated group compared to the untreated group (*P*<0.0001). In the atorvastatin 0.01, 0.5, and 20 μmol/L groups, it was significantly greater than the NMDA-treated group (*P*<0.1, 0.5, and 0.0001, respectively). The atorvastatin 20 μmol/L group showed significantly greater IR thickness compared to all other dose groups (*P*<0.0001).

The fractional thickness of the GCL within the IR was significantly lower in the NMDA group compared to the untreated group (*P*<0.001). In rats administered with 20 μmol/L of atorvastatin, the fractional GCL thickness within the IR was significantly greater compared to the NMDA-treated group (*P*<0.05), and the same observation was made for the atorvastatin 0.1 μmol/L group. Additionally, the atorvastatin 20 μmol/L group showed greater fractional thickness of GCL compared to the 0.5 and 1.0 μmol/L groups (*P*<0.01).

The number of retinal nuclei per 500 μm length of GCL was significantly lower in NMDA compared to the untreated group (*P*<0.0001). In contrast, the same in the atorvastatin 20 μmol/L group was greater by 1.81-fold compared to the NMDA-treated group (*P*<0.0001). In atorvastatin dose groups of 1.0, 0.5, and 0.1 μmol/L, the retinal cell density was 1.62, 1.69, and 1.52-fold greater than in the NMDA-treated group (*P*<0.001, <0.0001, and <0.01, respectively). Among various atorvastatin dose groups, retinal cell density was lowest in the group treated with 100 μmol/L compared to other dose groups (Figure 3D).

Effect of Atorvastatin on Retinal PPAR Expression

The retinal PPARα expression in NMDA-treated rats was significantly lower compared to the untreated group (*P*<0.0001). Treatment with atorvastatin increased the PPARα expression by 1.94-fold despite NMDA exposure (*P*<0.05). Moreover, the retinal PPARγ expression in the NMDA-treated group was significantly higher compared to the untreated group (*P*<0.0001). It was significantly lower in the atorvastatin-treated group than the NMDA-treated group by 2.44-fold (*P*<0.001). Additionally, the retina exposed to atorvastatin alone with NMDA exposure also showed significant lowering of PPARα and significant increase in PPARγ expression compared to the untreated group (*P*<0.0001 and 0.001, respectively; Figure 4).

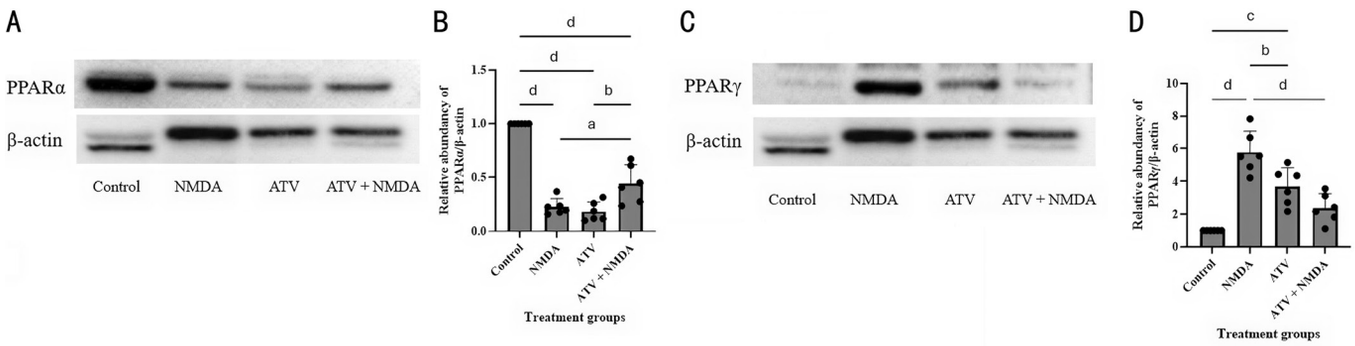


Figure 4 Effect of intravitreal ATV on retinal PPARs in the presence and absence of excitotoxic injury Statistical significance was analysed using one-way ANOVA with Bonferroni correction: [a]*P*<0.05, [b]*P*<0.01, [c]*P*<0.001, [d]*P*<0.0001. *n*=6. A: Western blot band showing PPARα expression; B: Densitometric estimation of PPARα expression; C: Western blot band showing PPARγ expression; D: Densitometric estimation of PPARγ expression. PPAR: Peroxisome proliferator-activated receptor; ANOVA: Analysis of variance; NMDA: N-methyl-D-aspartate; ATV: Atorvastatin.

DISCUSSION

In this study, first, we determined the affinity of six statins towards PPARα and PPARγ using *in-silico* methods utilizing artificial neural fully connected correlation networks based on multiple docking techniques. A comparative analysis of the data revealed several key findings. Atorvastatin and fluvastatin exhibited the highest affinity for the PPARα, with atorvastatin showing an affinity 2.80 times greater than that of fluvastatin. For the PPARγ, atorvastatin and pravastatin demonstrated the highest affinity, with atorvastatin's affinity being 2.60 times higher than that of pravastatin. Additionally, atorvastatin displayed a 1.23 times higher affinity for PPARγ compared to PPARα. Notably, atorvastatin surpassed all other statins by at least 4.30 times in terms of its combined pleiotropic effect on both PPARα and PPARγ. Hence, we further determined the anti-apoptotic effect of atorvastatin against NMDA-induced retinal cell apoptosis.

Our *in vivo* studies showed that the pre-treatment with atorvastatin reduces expression of the pro-apoptotic protein BAX and increases that of the anti-apoptotic protein Bcl2 in rat retinas exposed to NMDA. In line with our observations, atorvastatin was shown to attenuate the overexpression of BAX and induce the expression of Bcl2 mRNA in rat hippocampi subjected to ischemia-reperfusion injury. This effect of atorvastatin was associated with reduced neuronal apoptosis, improved mitochondrial function and reduced oxidative stress[36]. In another study that also used an ischemia-reperfusion model, increased Bcl2 expression was associated with reduced apoptosis and improved RGC survival after treatment with simvastatin[37-38]. Systemic delivery of statins was also shown to enhance RGC survival putatively through the modulation of heat shock proteins in the retina in response to ischemia-reperfusion injury[15].

In the current study, it was interesting to note that NMDA although increased BAX expression, the decline in Bcl2 was not significant. Nevertheless, the BAX/Bcl2 ratio indicated a shift of balance towards the greater activity of pro-apoptotic pathways. In atorvastatin-treated groups, not only was the BAX expression suppressed, but there was a marked increase in Bcl2 expression, which was even greater than in the untreated group, indicating its robust pro-survival effect. The same was also reflected in the retinal BAX/Bcl2 ratio. BAX, a pro-apoptotic protein, translocates from the cytoplasm to mitochondria in response to apoptotic stimuli and causes disruption of the mitochondrial inner transmembrane potential and release of cytochrome C. Cytochrome C forms apoptosomes and activates caspase-9, which in turn activates the caspase cascade leading to activation of caspase-3, the executioner caspase[39]. Bcl2, on the other hand, exerts anti-apoptotic effects by preventing the release of cytochrome C and, consequently, caspase activation[40]. Although apoptotic pathways may be triggered in a caspase-independent manner as well, studies have shown that RGC apoptosis associated with NMDA-induced excitotoxicity is largely mediated *via* caspase-3 activation and inhibitors of caspase-3 attenuate NMDA-induced neuronal apoptosis[41-43].

Therefore, considering the key role of caspase activation, we determined the effect of various doses of atorvastatin on NMDA-induced caspase-3 activation. Notably, all doses of atorvastatin suppressed the caspase-3 activation as reflected in the cleaved to pro-caspase ratio. In accordance with our observations, a previous study also reported a reduction in caspase-3 activation and increase in the Bcl2 expression by statins leading to retinal neuronal survival in an experimental model of retinal ischemia-reperfusion injury[37]. Hence, the dose-dependent variations in the anti-apoptotic effects of atorvastatin against NMDA-induced excitotoxicity were clearly evident in the current study. Its greatest anti-apoptotic effect was observed at a dose of 20 μmol/L compared to other doses, as reflected in BAX/Bcl2 as well as active/pro-

caspase-3 ratios. We used both of these ratios corresponding to the dose range used in this study to extrapolate and develop the log dose-response curve and calculate the ED_{95} for the anti-apoptotic effect of atorvastatin as a guide for further studies.

Although atorvastatin showed dose-dependent neuroprotective effect up to 20 μmol/L, at the higher concentration of 100 μmol/L, a similar response was not evident. We observed a U-shaped dose-response relationship. Such responses are frequently described in neuropharmacology when drug concentrations increase beyond the optimal range[44]. This may be attributed to concentration-dependent cellular toxicity through excessive inhibition of the mevalonate pathway, leading to reduced essential isoprenoid intermediate, impairment of mitochondrial function, increased oxidative stress and disruption of membrane cholesterol homeostasis[45].

Although statins, including atorvastatin, can permeate into the retina after systemic administration due to lipophilicity, the amount reaching the retinal tissue is relatively limited. Previous studies have demonstrated the presence of atorvastatin in the retina following systemic administration, indicating that it can cross the blood-retinal barrier[46]. In the present study, intravitreal administration was chosen to deliver atorvastatin directly to the retina and to reduce the variability associated with systemic drug distribution and retinal penetration. This approach also allowed us to evaluate the local dose-dependent neuroprotective effects of atorvastatin against NMDA-induced retinal excitotoxicity. However, as systemic or topical administration is more relevant to the clinical use of atorvastatin for glaucoma, future studies using systemic and topical administration would be valuable in determining the translational relevance of these findings.

Atorvastatin was given before NMDA exposure as the aim of this study was to examine its potential to protect the retina from excitotoxic injury, rather than to reverse damage that had already occurred. Pretreatment allowed atorvastatin to be present in the retinal tissue before the excitotoxic process was initiated by NMDA and enabled us to assess whether it could reduce the subsequent neuronal injury and apoptosis. This approach is supported by previous experimental work showing greater protection against NMDA-induced retinal apoptosis with pretreatment than with co- or post-treatment[35]. Moreover, the neuroprotection in response to pretreatment is specifically relevant to chronic progressive diseases like glaucoma due to its ability to potentially halt the disease progression.

To corroborate the anti-apoptotic effects of atorvastatin, we measured the extent of RGC survival by evaluating the RBPMS expression in rat retina. RBPMS, a member of the RNA recognition motif (RRM) family of RNA-binding proteins, is expressed exclusively by RGCs in multiple mammalian species, and its downregulation is associated with degenerative loss of RGCs[47]. The current study showed a significantly greater RBPMS protein expression in rat retinas that received atorvastatin 20 μmol/L pre-treatment compared to those treated with NMDA alone, suggesting enhanced RGC survival in response to atorvastatin pre-treatment. In accordance with our findings, a previous study reported that statins promote the survival of RGCs and reduce apoptosis in a rat model of chronic ocular hypertension[37]. The retinal morphological observations made in our study align with the anti-apoptotic effect of atorvastatin and its effect on RGC survival. A reduced GCL and IR thickness and retinal cell density indicated the excitotoxicity-induced loss of neuronal cells in GCL, and this was in accordance with previous studies[35,48]. In atorvastatin-treated groups, we observed that the thickness of GCL, as well as the IR, was restored presumably due to lesser apoptotic loss of neurons as well as surviving RGCs. Importantly, to eliminate the possible effect of the shrinkage of GCL in response to NMDA exposure, we calculated nuclear density over a specified length rather than the specified area. Nevertheless, an increased retinal cell density was evident in all atorvastatin-treated groups, with the most prominent effect at a 20 μmol/L dose.

Considering the affinity of atorvastatin for PPARα and PPARγ receptors revealed by *in-silico* studies, in the next set of experiment we used the 15 μmol/L doses of atorvastatin (~ED_{95}) with or without NMDA exposure and measured its effects on retinal expression of both PPARs. PPAR activation has been shown to suppress mitochondrial apoptotic cascade, resulting in decreased BAX/Bcl2 ratio, reduced cytochrome c release, reduced apoptosome formation and prevention of downstream cleavage of caspase-3. In fact, PPARγ activation was shown to protect mitochondrial membrane potential and exert an anti-apoptotic effect by upregulating Bcl-2 and preventing caspase activation[49-50].

In the current study, we observed a significant suppression of PPARα expression 7d post-NMDA exposure, while pre-treatment with atorvastatin was associated with an increased PPARα expression. The overexpression of PPARα has earlier been shown to protect retinal cells against hypoxic injury by reducing oxidative stress[51]. PPARα activation by PPARα agonist has also been shown to protect RGCs by suppressing NMDA-induced inflammation through inhibition of nuclear factor kappa B and c-Jun expression[52-53]. Considering the high affinity of atorvastatin for PPARα as shown by *in-silico* studies, our observation of inhibition of NMDA-induced suppression of PPARα, therefore, seems to be in line with the earlier observations. The nature of interaction between atorvastatin and PPARα, however, remains unclear. Furthermore, current study could not rule out if this change in

the expression of PPARα involves other pathways leading to an indirect effect of atorvastatin. Unexpectedly, we observed significant downregulation of PPARα expression in rat retinas that were treated with atorvastatin in the absence of NMDA-induced injury. Although the precise explanation for this finding remains unclear, observations from previous studies suggest a negative feedback loop that autoregulates the PPARα expression. It has been observed that activation of PPARα increases thioredoxin expression, which in turn inhibits PPARα expression and activation[54]. Since PPARα activity has prominent physiological functions including regulation of excitatory neurotransmission, this negative-feedback loop, by inhibiting excessive PPARα activity in uninjured retinas, is likely to be a protective response for maintaining tissue homeostasis. Considering the pleiotropic actions of atorvastatin, the involvement of other molecular pathways in this downregulation of PPARα in the absence of NMDA-induced injury could not be ruled out.

In contrast to the effects of NMDA on PPARα expression, we observed a significant increase in the expression of PPARγ, 7d post-NMDA exposure. Previous studies have shown that NMDA exposure enhances the expression of PPARγ in microglia. It was proposed that increased expression of inflammatory cytokines due to excitotoxic injury activates signal transducer and activator of transcription 6 (STAT6), which in turn promotes PPARγ expression and "healing" phenotype of microglia. The reprogramming of microglia from a pro-inflammatory to a ''healing'' phenotype is proposed as a self-defense response protecting neurons from further injury[55-56]. In neuronal tissue, PPARγ expression is largely localized to the microglia and astrocytes and plays a significant role in the inflammatory responses. Pre-treatment with atorvastatin seems to protect against inflammation and oxidative stress response to NMDA exposure. Hence, compared to the NMDA-treated group, in the atorvastatin pre-treatment group, a relatively lower PPAR expression is triggered for further neuronal protection due to the initial relatively lower severity of inflammation and oxidative stress. Greater PPARγ expression in the atorvastatin treatment group without NMDA exposure compared to control also aligns with its possible PPARγ agonistic activity, though an indirect effect could not be ruled out. In line with our observations, it was reported that the lack of PPARγ activity aggravates neuronal excitability and excitotoxicity[57]. One of the studies has shown that endogenous PPARγ ligand, as well as PPARγ agonist, ciglitazone, protect against neuronal cell death caused by glutamate and NMDA in culture and animal models. This neuroprotective effect was reversed by selective pharmacologic antagonists of PPARγ as well as anti-PPARγ antibodies. Interestingly, one of the studies showed that PPARγ agonists did not prevent the rise in Ca^{2+} concentration till 75s post-NMDA application. Hence, it is likely that the protective effect of PPARγ *via* inhibition of Ca^{2+} overload may be delayed. Alternatively, activation of other protective pathways, such as those causing increased expression of antioxidants and reduced oxidative stress, may underlie the pro-survival effects[58].

It is interesting to note that at the same time point following NMDA exposure, opposite trends were observed for the expression of PPARα and PPARγ despite the reported anti-inflammatory and anti-oxidative effects of activation of both receptors. The difference may result from the extent of activation of each of the PPAR subtypes by the given atorvastatin concentration due to differences in affinity or differential activation of alternate pathways affecting PPAR expression. Further, to the best of our knowledge, the relative extent of involvement of PPARs in response to NMDA exposure has not been investigated. It is also noteworthy that we measured the PPARs expression only at 7d post-NMDA exposure; therefore, if there are differences in the time-dependent activation of two PPAR subtypes under these experimental conditions remains to be investigated. The current study also did not determine the pathways leading to changes in PPAR expression following atorvastatin treatment. Moreover, the nature of possible direct interactions of atorvastatin with PPAR remains unclear. Nevertheless, the current study clearly demonstrates an altered PPAR expression in response to NMDA exposure and inhibition of these alterations by atorvastatin.

In conclusion, current study showed that among several statins, atorvastatin has the maximum affinity towards PPARα and PPARγ. The intravitreal administration of atorvastatin prevents NMDA-induced retinal cell apoptosis and promotes RGC survival in rats. This effect of atorvastatin is associated with inhibition of NMDA-induced changes in retinal PPARα and PPARγ expression.

ACKNOWLEDGEMENTS

Authors' Contributions: All authors contributed to the study conception and design. Material preparation, data collection and analysis were performed by Wong JY, Jaiprakash H, Agarwal R, Iezhitsa I. The first draft of the manuscript was written by Wong JY, Jaiprakash H, Agarwal R, Iezhitsa I, and all authors commented on previous versions of the manuscript. All authors read and approved the final manuscript.

Data Availability Statement: The data that support the findings of this study are available from the corresponding author upon reasonable request.

AI-Generated Content Disclosure: AI was used only for correcting sentence structures at places.

Foundations: Supported by IMU University [No.PHMS I-2023 (01); No.MMHS I-2023(01)]; The *in-silico* research

was conducted as part of the state assignment from the Ministry of Health of the Russian Federation (No.23022400009-9).

Conflicts of Interest: Wong JY, None; **Jaiprakash H,** None; **Agarwal R,** None; **Iezhitsa I,** None; **Krishnappa P,** None; **Wong ST,** None; **Perfilev MA,** None; **Vassiliev PM,** None.

REFERENCES

1 Lukasiewicz PD. Synaptic mechanisms that shape visual signaling at the inner retina. *Prog Brain Res* 2005;147:205-218.

2 Casson RJ. Possible role of excitotoxicity in the pathogenesis of glaucoma. *Clin Exp Ophthalmol* 2006;34(1):54-63.

3 Kalia LV, Kalia SK, Salter MW. NMDA receptors in clinical neurology: excitatory times ahead. *Lancet Neurol* 2008;7(8):742-755.

4 Dong CJ, Guo Y, Agey P, *et al*. Alpha2 adrenergic modulation of NMDA receptor function as a major mechanism of RGC protection in experimental glaucoma and retinal excitotoxicity. *Invest Ophthalmol Vis Sci* 2008;49(10):4515-4522.

5 Yao F, Zhang X, Yao X, *et al*. Peroxisome proliferator-activated receptor α activation protects retinal ganglion cells in ischemia-reperfusion retinas. *Front Med (Lausanne)* 2021;8:788663.

6 Zhang S, Gu H, Hu N. Role of peroxisome proliferator-activated receptor *γ* in ocular diseases. *J Ophthalmol* 2015;2015:275435.

7 Zhu J, Zhang J, Ji M, *et al*. The role of peroxisome proliferator-activated receptor and effects of its agonist, pioglitazone, on a rat model of optic nerve crush: PPARγ in retinal neuroprotection. *PLoS One* 2013;8(7):e68935.

8 Grip O, Janciauskiene S, Lindgren S. Atorvastatin activates PPARγ and attenuates the inflammatory response in human monocytes. *Inflamm Res* 2002;51(2):58-62.

9 Morishita S, Oku H, Horie T, *et al*. Systemic simvastatin rescues retinal ganglion cells from optic nerve injury possibly through suppression of astroglial NF-κB activation. *PLoS One* 2014;9(1):e84387.

10 Stein JD, Newman-Casey PA, Talwar N, *et al*. The relationship between statin use and open-angle glaucoma. *Ophthalmology* 2012;119(10):2074-2081.

11 Leung DYL, Li FCH, Kwong YYY, *et al*. Simvastatin and disease stabilization in normal tension glaucoma: a cohort study. *Ophthalmology* 2010;117(3):471-476.

12 Whigham B, Oddone EZ, Woolson S, *et al*. The influence of oral statin medications on progression of glaucomatous visual field loss: a propensity score analysis. *Ophthalmic Epidemiol* 2018;25(3):207-214.

13 Yuan Y, Xiong R, Wu Y, *et al*. Associations of statin use with the onset and progression of open-angle glaucoma: a systematic review and meta-analysis. *EClinicalMedicine* 2022;46:101364.

14 Krempler K, Schmeer CW, Isenmann S, *et al*. Simvastatin improves retinal ganglion cell survival and spatial vision after acute retinal ischemia/reperfusion in mice. *Invest Ophthalmol Vis Sci* 2011;52(5):2606-2618.

15 Schmeer C, Gámez A, Tausch S, *et al*. Statins modulate heat shock protein expression and enhance retinal ganglion cell survival after transient retinal ischemia/reperfusion *in vivo*. *Invest Ophthalmol Vis Sci* 2008;49(11):4971-4981.

16 The Association for Research in Vision and Opthamology. ARVO Statement for the Use of Animals in Ophthalmic and Vision Research. 2021.

17 PerkinElmer/Chemistry: Official website of PerkinElmer, Inc. (n.d.). Available on: 2023 May 16. https://www.perkinelmer.com/product/chemoffice-chemoffice

18 MarvinSketch: Official website of ChemAxon Kft. 2023. https://chemaxon.com/marvin

19 MOPAC: Official website of J.J.P. Stewart, Stewart Computational Chemistry. (n.d.). Available on: 2023 June 20. http://openmopac.net

20 Vasilyev P, Kochetkov A, Spasov A, *et al*. The energy spectrum of multiple docking as a multi-dimensional metric of the affinity of chemical compounds to pharmacologically relevant bio-targets. *Volgogr J Med Res* 2021;3(4):57-61.

21 Trott O, Olson AJ. AutoDock Vina: improving the speed and accuracy of docking with a new scoring function, efficient optimization, and multithreading. *J Comput Chem* 2010;31(2):455-461.

22 Microsoft Office: Official website of Microsoft, Inc. 2023. https://www.office.com/

23 DrugBank: Official website of the University of Alberta (Canada). (n.d.). Available on: 2024 March 4. https://www.drugbank.com/

24 IUPHAR/BPS Guide to PHARMACOLOGY: Official website of the International Union of Basic and Clinical Pharmacology and the British Pharmacological Society. 2024. https://www.guidetopharmacology.org/

25 UniProt. UniProt: Official website of the UniProt Consortium (Switzerland, UK, USA). 2024. https://www.uniprot.org/uniprotkb/

26 PDBe. PDBe: Protein Data Bank in Europe: Official website of the European Molecular Biology Laboratory at the European Bioinformatics Institute (UK). 2024. https://www.ebi.ac.uk/pdbe/

27 Hebb D. *Organization of Behavior*. New York: John Wiley AND Sons; 1949.

28 Hopfield JJ. Neural networks and physical systems with emergent collective computational abilities. *Proc Natl Acad Sci U S A* 1982;79(8):2554-2558.

29 Hilbe JM. STATISTICA 7: an overview. *Am Stat* 2007;61:91-94.

30 Jin Y, Sui HJ, Dong Y, *et al*. Atorvastatin enhances neurite outgrowth in cortical neurons *in vitro via* up-regulating the Akt/mTOR and Akt/GSK-3β signaling pathways. *Acta Pharmacol Sin* 2012;33(7):861-872.

31 Wang H, Chen Y, Li P, *et al*. Biphasic effects of statins on neuron cell functions under oxygen-glucose deprivation and normal culturing conditions *via* different mechanisms. *Pharmacol Res Perspect* 2022;10(5):e01001.

32 Lambuk L, Jafri AJA, Iezhitsa I, *et al*. Dose-dependent effects of NMDA on retinal and optic nerve morphology in rats. *Int J Ophthalmol* 2019;12(5):746-753.

33 Mohammed Irfan AMS, Geoffrey S, Htet H, *et al*. N-methyl- d-aspartate-induced excitotoxicity and its impact on the renin–angiotensin system in retinal tissue. *J Ocul Pharmacol Ther* 2025;41(2):79-86.

34 Arfuzir NNN, Lambuk L, Jafri AJA, *et al*. Protective effect of magnesium acetyltaurate against endothelin-induced retinal and optic nerve injury. *Neuroscience* 2016;325:153-164.

35 Jafri AJA, Agarwal R, Iezhitsa I, *et al*. Protective effect of magnesium acetyltaurate and taurine against NMDA-induced retinal damage involves reduced nitrosative stress. *Mol Vis* 2018;24:495-508.

36 Yadollah-Damavandi S, Sharifi ZN, Arani HZ, *et al*. Atorvastatin prevents the neuron loss in the hippocampal dentate gyrus region through its anti-oxidant and anti-apoptotic activities. *CNS & Neurol Disord-Drug Targets* 2021;20(1).

37 Ko ML, Chen CF, Peng PH, *et al*. Simvastatin upregulates Bcl-2 expression and protects retinal neurons from early ischemia/reperfusion injury in the rat retina. *Exp Eye Res* 2011;93(5):580-585.

38 Zhang Y, Zhang Z, Yan H. Simvastatin inhibits ischemia/reperfusion injury-induced apoptosis of retinal cells *via* downregulation of the tumor necrosis factor-α/nuclear factor-κB pathway. *Int J Mol Med* 2015;36(2):399-405.

39 Finucane DM, Bossy-Wetzel E, Waterhouse NJ, *et al*. Bax-induced caspase activation and apoptosis *via* cytochromec release from mitochondria is inhibitable by Bcl-xL. *J Biol Chem* 1999;274(4):2225-2233.

40 Yang J, Liu X, Bhalla K, *et al*. Prevention of apoptosis by Bcl-2: release of cytochrome c from mitochondria blocked. *Science* 1997;275(5303):1129-1132.

41 Du Y, Bales KR, Dodel RC, *et al*. Activation of a caspase 3-related cysteine protease is required for glutamate-mediated apoptosis of cultured cerebellar granule neurons. *Proc Natl Acad Sci U S A* 1997;94(21):11657-11662.

42 Seki M, Soussou W, Manabe SI, *et al*. Protection of retinal ganglion cells by caspase substrate-binding peptide IQACRG from N-methyl-D-aspartate receptor-mediated excitotoxicity. *Invest Ophthalmol Vis Sci* 2010;51(2):1198-1207.

43 Zhou X, Hollern D, Liao J, *et al*. NMDA receptor-mediated excitotoxicity depends on the coactivation of synaptic and extrasynaptic receptors. *Cell Death Dis* 2013;4(3):e560.

44 Calabrese EJ. Hormesis and medicine. *Br J Clin Pharmacol* 2008;66(5):594-617.

45 Golomb BA, Evans MA. Statin adverse effects: a review of the literature and evidence for a mitochondrial mechanism. *Am J Cardiovasc Drugs* 2008;8(6):373-418.

46 Mast N, Bederman IR, Pikuleva IA. Retinal cholesterol content is reduced in simvastatin-treated mice due to inhibited local biosynthesis albeit increased uptake of serum cholesterol. *Drug Metab Dispos* 2018;46(11):1528-1537.

47 Rodriguez AR, de Sevilla Müller LP, Brecha NC. The RNA binding protein RBPMS is a selective marker of ganglion cells in the mammalian retina. *J Comp Neurol* 2014;522(6):1411-1443.

48 Lambuk L, Jafri AJA, Arfuzir NNN, *et al*. Neuroprotective effect of magnesium acetyltaurate against NMDA-induced excitotoxicity in rat retina. *Neurotox Res* 2017;31(1):31-45.

49 Jin YN, Hwang WY, Jo C, *et al*. Metabolic state determines sensitivity to cellular stress in Huntington disease: normalization by activation of PPARγ. *PLoS One* 2012;7(1):e30406.

50 Wu JS, Lin TN, Wu KK. Rosiglitazone and PPAR-gamma overexpression protect mitochondrial membrane potential and prevent apoptosis by upregulating anti-apoptotic Bcl-2 family proteins. *J Cell Physiol* 2009;220(1):58-71.

51 Moran E, Ding L, Wang Z, *et al*. Protective and antioxidant effects of PPARα in the ischemic retina. *Invest Ophthalmol Vis Sci* 2014;55(7):4568-4576.

52 Fujita N, Sase K, Tsukahara C, *et al*. Pemafibrate prevents retinal neuronal cell death in NMDA-induced excitotoxicity *via* inhibition of p-c-Jun expression. *Mol Biol Rep* 2021;48(1):195-202.

53 Sun Y, Alexander SPH, Garle MJ, *et al*. Cannabinoid activation of PPAR alpha; a novel neuroprotective mechanism. *Br J Pharmacol* 2007;152(5):734-743.

54 Liu GH, Qu J, Shen X. Thioredoxin-mediated negative autoregulation of peroxisome proliferator-activated receptor alpha transcriptional activity. *Mol Biol Cell* 2006;17(4):1822-1833.

55 Huang JT, Welch JS, Ricote M, *et al*. Interleukin-4-dependent production of PPAR-gamma ligands in macrophages by 12/15-lipoxygenase. *Nature* 1999;400(6742):378-382.

56 Ting SM, Zhao X, Zheng X, *et al*. Excitatory pathway engaging glutamate, calcineurin, and NFAT upregulates IL-4 in ischemic neurons to polarize microglia. *J Cereb Blood Flow Metab* 2020;40(3):513-527.

57 Hung TY, Chu FL, Wu DC, *et al*. The protective role of peroxisome proliferator-activated receptor-gamma in seizure and neuronal excitotoxicity. *Mol Neurobiol* 2019;56(8):5497-5506.

58 Zhao X, Ou Z, Grotta JC, *et al*. Peroxisome-proliferator-activated receptor-gamma (PPARγ) activation protects neurons from NMDA excitotoxicity. *Brain Res* 2006;1073:460-469.